



Structural and Electronic Characterization of III-V Binary Semiconductors: A DFT Approach

Abdul Wakil

[Department of Physics, Islamia College University, Peshawar, 25120, Pakistan]

Article Information

Article Type: Research Article

Dates:

Received: 07 February 2024

Revised: 24 March 2024

Accepted: 15 April 2024

Available online:

Copyright:

This work is licensed under Creative
Common license and ©2024 All rights
reserved Innovate Humanity Publisher

ABSTRACT

This work investigates the structural and electrical characteristics of III-V binary semiconductors using elements from groups V and III of the periodic table. This work aims to compute accurate bulk moduli, electronic band gaps, and lattice constants in the zinc-blende structure using Density Functional Theory in conjunction with the full-potential linearized augmented plane wave approach and Wu-Cohen generalized gradient approximation (GGA) in conjunction with the modified Becke-Johnson potential. These parameters are necessary to evaluate the effects of changing the anions and cations in the series. The findings reveal that with the introduction of heavier anions and cations, lattice constants increase while bulk moduli decrease, consistent with periodic properties. The calculated electronic band gaps closely match experimental results, affirming the accuracy of the selected DFT approaches. This detailed evaluation provides a deeper understanding of the material properties of III-V binary semiconductors, including their elastic characteristics like elastic constants and Young's modulus. These insights confirm the materials' potential for advanced electronic and optoelectronic applications. The study not only corroborates previous theoretical and experimental work but also expands our knowledge of semiconductor behavior when modified at the elemental level, paving the way for future research in this field.

Keywords: III-V binary semiconductors, Density Functional Theory (DFT), Elastic properties, Electronic band gaps

INTRODUCTION

One element from group III and one element from group V of the periodic table are present in the group III-V binary semiconductors[1]. Compared to silicon (Si), several of the compounds in this family exhibit wider band gaps and better electron mobility. These characteristics allow them to function faster and at a greater temperature in power devices[2]. Additionally, they are extensively used in filters, integrated circuits, modulators, lasers, photo detectors, and light emitting diodes. Because it is the softest and most stable of the BN polymorphs, hexagonal graphite is added to cosmetic items and used as a lubricant. The diamond-analogous cubic variation is known as c-BN. The normal form's hardness is only surpassed by diamond's, but when it is manufactured with a nanostructure dominated by fine twin domains with an average thickness of less than 3.8 nm, it is harder than synthetic diamond. One type of direct band gap semiconductor is boron bismuth. For low-temperature thermo-photovoltaic cells, gallium antimonide GaSb is a good material because of its simple cell technology, which results in higher efficiency than Si thermo-photovoltaic cells. Microwave devices and optoelectronic materials are made of indium nitride (InN). InN's remarkable development causes it to expand in the ZB structure[3]. Because of its higher electron velocity than that of silicon and arsenide, two other semiconductors Electronics that require high power and high frequency employ indium phosphide. Because of its indirect band gap, optoelectronic devices are just as powerful as laser diodes. The binary semiconductor Indium Antimonide has a straight band gap. Owing to its narrow gap, infrared astronomy, infrared homing missile guidance systems, and cameras all use infrared detectors[4]. At wavelengths between 1 and 5 μm , indium antimonide detectors exhibit high sensitivity. The quantum well is an InSb- AlInSb structure. One material with a direct band gap semi conductor is indium arsenide, or InAs [5]. Indium arsenide is utilised in the development of infrared detectors, with a wavelength range of 1-3.8 μm . Photovoltaic photodiodes are frequently used as the detectors. Diode lasers are another application for it. The ground state phase is home to thallium nitride. Thallium-V-based optoelectronic devices have benefits over II-VI semiconductor devices because to the -V's excess advantages. This makes them interesting for use in near-infrared optical communication systems (laser diodes, detectors). The goal of this study is to determine the III-V compounds' structure and elastic properties utilizing the theoretical framework of density functional theory. Every computation is based on the functional form of Wu-Kohan and the FP-LAPW approach. Band structure and state density

of the compounds are used to characterize structural features. The compounds' elastic nature is examined in relation to the imaginary and real components of the dielectric function. Young modulus, bulk modulus, shear modulus, elasticity, stress, strain, and the modulus of elasticity are all examples of elastic constants.

Methodology

In physics and chemistry, density functional theory is a quantum mechanical modelling technique used to study the electronic structure (essentially the ground state) of many-body systems, specifically atoms, molecules, and phases. It is used by quantum chemists to simulate the energy surface of molecules. We investigate the binding energy, superconductivity, intense laser pulses, relativistic effect in heavy elements, band structure, and magnetic characteristics of alloys by applying the general density functional theory. The two Hohenberg–Kohn theorems (H–K) make up DFT. For non-degenerate ground states without a magnetic field, the first H–K theorem applies. For self-consistent-field electronic structure simulations of the ground-state characteristics of atoms, molecules, and solids, Kohn-Sham density functional theory is extensively employed. The ground state density of a non-interacting electron system can be found using the Schrodinger wave equation, which is developed by applying the variational principle to the non-interacting electron system. The fundamental idea behind the Kohn-Sham (KS) system is to link an artificial system of electrons that is not interacting with the real system of electrons in order to obtain the same ground state energy and density as the interacting electrons. Since the electrons in this non-interacting Kohn-Sham (KS) system do not behave like charge particles, they cannot, by definition, interact with one another via the Coulomb interaction. Improving the approximation of the exchange correlation functional, $E_{xc}[\rho(r)]$, of the Kohn-Sham equations was the primary goal of modern DFT. The Local Density Approximation (LDA) was the most straightforward of all three approximations. The primary idea of the LDA was to use the exchange correlation hole corresponding to the homogeneous electron gas at each location in space with the same density and treat an inhomogeneous electric field as a locally inhomogeneous field. The exchange correlation energy density is constant at every point in the homogeneous electron plasma at the same density, and the exchange correlation energy can be computed by integrating across the whole surface. The electronic density $\rho(r)$ describes any actual, non-uniform system, and at each 'r', there is an exchange correlation energy denoted by $\epsilon_{xc}[\rho(r)]$.

Two zones can be distinguished in an atomic system: the tiny volume that the atom occupies and the area surrounding this volume. GGA creates the exchange correlation that accounts for the density in the adjacent volume as well as inside the tiny volume. The outcome will be non-uniform if the exchange correlation energy is not uniform. We employ the gradient and higher derivatives of the total charge density to express this variation. The Generalised Gradient Approximation is utilised to remedy this deviation. Different Generalized Gradient Approximation parameters have been proposed and tested on many kinds of materials. The Generalized Gradient Approximation yields considerably superior results than the Local Density Approximation (LDA) due to the latter's leakage of light atom, element, and solid ground state properties. In equilibrium, the generalized gradient approximation yields a larger lattice parameter than the local density approximation. Because it can freely unite the density gradient and has a unique definition of ϵ_{xc} Local density exchange correlation with a single volume, the Generalized Gradient Approximation has multiple versions. Additionally, additional experimental specification is needed when using the Generalized Gradient Approximation computation instead of the ab-initio method. In practice, we fit experimental data to a Generalized Gradient Approximation functional with specific parameters; the best findings are fixed, and the functional is applied to solids.

Results and Discussion

The volume optimization approach is used to compute the structural characteristics of the III–V compounds XY (X=B, Al, Ga, In, Tl; Y=N, P, As, Sb, Bi) in the zincblende phase. Fig. (1) depicts the zincblende structure (space group #216). The unit cell's (0, 0, 0) corner has X cations, and its (0.25, 0.25, 0.25) diagonal contains Y anions. The unit cell volume is changed during the volume optimization process, and the corresponding change in the unit cell energy is recorded. The Birch-Morang equation of state fits the unit cell volume vs the unit cell energy for each component. Fig. 2 displays the optimisation plot of BN. The graphic illustrates how unit cell energy drops and achieves its minimal value as volume increases. The volume that corresponds to this energy is referred to as the ground state optimum volume, and it is known as the ground state unit cell energy[6]. Energy in the unit cell increases once more beyond the optimal volume. For the III–V binary compounds, the ground state structural parameters are computed and shown in Table 1. The table shows that our estimates closely match previous projected results and the existing experimental data. For the first time, some of the compounds TlSb and TlBi are

described. Furthermore, it is seen that the lattice constant rises when cations are changed from B to Tl and anions are changed from N to Bi. By shifting the anions or cations from the top to the bottom of the periodic table, bulk modulus lowers[7]. As a result, as cations or anions move from top to bottom of the periodic table, III–V's hardness falls and its compressibility rises. The ground state energy of unit cells is likewise increasing in the same direction. Since, as far as we are aware, neither experimental nor theoretical research has been done on any of these chemicals, this study can serve as a helpful guide for future theoretical and experimental studies[8].

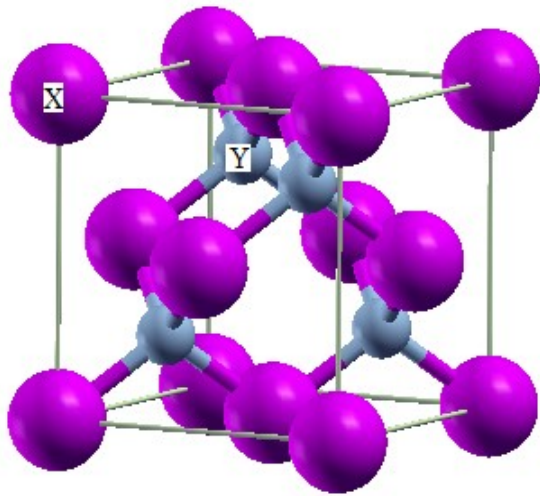


Fig.1. Zincblende crystal structure

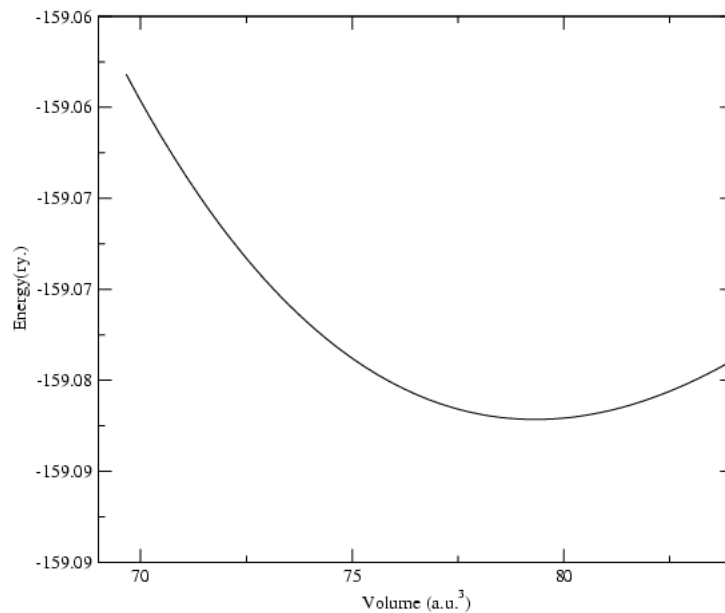


Fig.2. Optimization plot of BN in zincblende phase

The elastic constants The elastic nature of III-V compounds is characterized by the calculation of their C_{ij} . These constants are crucial in giving useful details on the stiffness and stability of materials. Utilizing a technique created by Charpin and incorporated into the WIEN2K algorithm, we computed the components of the stress tensor for tiny strains in order to compute them using numerical first principle calculations. We just need to compute the three independent elastic parameters C_{11} , C_{12} , and C_{44} to fully characterize the mechanical properties of the compounds under study because they have cubic symmetry. Therefore, in order to find all of these constants, a set of three equations is required. The Young's modulus (E) provides useful information regarding the material's stiffness [9]. It indicates how stiff a particular material is when it is higher. More information about the bonding force characteristic can be found in Poisson's ratio than in any other elastic feature. The lower and upper bounds for central force solids are, respectively, 0.25 and 0.5. The interatomic forces are important in these compounds because the computed Poisson's ratio falls between these values. It is well known that a high resistance to bond bending or bond angle distortion is implied by a low Kleinman parameter value, and vice versa. Poisson's ratio (ν), Cauchy pressure ($C_{12}-C_{44}$), and Pugh's index of ductility (B/G) are measurements that help us determine if a material is brittle or ductile. A measure of ductility is the Cauchy's pressure, which is the difference between two specific elastic constants ($C_{12}-C_{44}$). A positive or negative pressure indicates that the material is predicted to be brittle or ductile. Here, the fact that all of the compounds have positive values for Cauchy's pressure emphasises how ductile they are. The ratio of (B/G) is another measure of ductility. Pugh's ratio states that the ductile (brittle) or high (low) B/G ratio corresponds to the properties of the materials. We can also consult Frantsevich et al., who differentiate between brittleness and ductility in materials using Poisson's ratio (ν). The Frantsevich rule states that a material's critical value is 0.26. When a material's Poisson's ratio is less than 0.26, it is considered brittle; otherwise, it exhibits ductile behavior. Since the computed Poisson's values in this case are more than 0.26, the compounds are classified as ductile materials[10].

Table 1: Young's modulus (E), shear modulus (G), the Poisson's ratio (ν), the anisotropy Factor (A) and Pugh's index of ductility (B/G)

Compounds	E	G	ν	A	B/G
-----------	-----	-----	-------	-----	-------

BN	821.4	363.4	0.130	1.48	1.018
BP	378.99	172.65	0.108	1.5	0.940
Bas	303.49	136.3	0.113	0.89	0.959
BSb	132.36	52.27	0.266	2.165	1.804
BBi	173.71	-31.41	0.7723	-4.1644	-2.172
AlN	309.25	125.86	0.228	3.5	1.50
AlP	133.18	54.075	0.231	2.65	1.529
AlAs	113.58	46.66	0.217	2.11	1.433
AlSb	70.8	28.02	0.358	2.37	1.77
AlBi	61.980	24.75	0.252	6.92	1.683
GaN	247.9	98.2	0.262	21.9	1.771
GaP	113.36	45.05	0.258	2.64	1.734
GaAs	113.7	48.22	0.178	0.88	1.223
GaSb	86.7	36.95	0.173	1.28	1.196
GaBi	58.55	23.99	0.44	0.27	1.453
InN	1241.48	329.452	-.15122	1.341	3.627
InP	104.55	43.115	0.212	0.7	1.405
InAs	63.43	24.74	0.281	3.23	1.95
InSb	44.65	17.135	0.303	0.82	2.209
InBi	79.177	37.74	0.04899	0.1905	0.775
TlN	88.166	-33.1218	0.330	-0.6355	-2.623
TlP	56.43	21.63	0.309	0.5	2.289
TlAs	68.4	28.195	0.217	0.64	1.437
TlSb	61.73	27.96	0.104	0.7	0.928
TlBi	-45.69	-12.98	0.760	-25.04	-2.254

Conclusion

Wu-Cohen GGA and mBJ potentials are combined with the FP-LAPW technique to predict the structural and electrical properties of XY (X=B, Al, Ga, In, Tl; Y=N, P, As, Sb, Bi) compounds in zincblende phase. The main conclusions show that the lattice constant rises and the bulk modulus decreases as the anion is changed from N to Bi from top to bottom of the periodic table.

The pattern remains the same when the cations are changed from B to Tl. The electronic band gaps of the compounds are far closer to the experimental results than previous theoretical estimations. Future studies on these compounds can be guided by the findings of this work.

Acknowledgements: Acknowledgments and Reference heading should be left justified, bold, with the first letter capitalized but have no numbers. Text below continues as normal.

Author contributions: All authors equally contributed to this study

Ethical Statement:

Competing Interests: The author declares that this work has no competing interests.

Grant/Funding information: The author declared that no grants supported this work.

Data Availability Statement: The associated data is available upon request from the corresponding author.

REFERENCES

1. Vyas, K., et al., *Group III-V semiconductors as promising nonlinear integrated photonic platforms*. Advances in Physics: X, 2022. **7**(1): p. 2097020.
2. Sun, M., et al., *Ultrahigh carrier mobility in the two-dimensional semiconductors B8Si4, B8Ge4, and B8Sn4*. Chemistry of Materials, 2021. **33**(16): p. 6475-6483.
3. Maji, B. and R. Chattopadhyay, *Design and optimization of high efficient GaSb homojunction solar cell using GaSb intrinsic layer*. Microsystem Technologies, 2021. **27**(9): p. 3589-3598.
4. Jin, Z., *Arsenide Nanowire Based Quantum Materials for Advanced Photonics*. 2020: Lancaster University (United Kingdom).
5. Diakite, Y.I., et al., *First Principle Calculation of Accurate Electronic and Related Properties of Zinc Blende Indium Arsenide (zb-InAs)*. Materials, 2022. **15**(10): p. 3690.
6. Xu, K., et al., *Ground-state electron transfer in all-polymer donor–acceptor heterojunctions*. Nature materials, 2020. **19**(7): p. 738-744.
7. Martelli, F., *Electrolyte Permeability in Plastic Ice VII*. The Journal of Physical Chemistry B, 2023. **127**(30): p. 6734-6742.
8. Chen, F., et al., *Atomic-level charge separation strategies in semiconductor-based photocatalysts*. Advanced Materials, 2021. **33**(10): p. 2005256.
9. Guimarães, C.F., et al., *The stiffness of living tissues and its implications for tissue engineering*. Nature Reviews Materials, 2020. **5**(5): p. 351-370.
10. Daoud, S., et al., *High-pressure effect on elastic constants and their related properties of MgCa intermetallic compound*. physica status solidi (b), 2020. **257**(6): p. 1900537.